



**University of
Zurich**^{UZH}

**Zurich Open Repository and
Archive**

University of Zurich
University Library
Strickhofstrasse 39
CH-8057 Zurich
www.zora.uzh.ch

Year: 2014

Finite top-mass effects in gluon-induced Higgs production with a jet-veto at NNLO

Neumann, Tobias ; Wiesemann, Marius

Abstract: Effects from a finite top quark mass on the $H + n$ -jet cross section through gluon fusion are studied for $n = 0, 1$ at NNLO/NLO QCD. For this purpose, sub-leading terms in $1/m_t$ are calculated. We show that the asymptotic expansion of the jet-vetoed cross section at NNLO is very well behaved and that the heavy-top approximation is valid at the five permille level up to jet-veto cuts of 300 GeV. For the inclusive Higgs+jet rate, we introduce a matching procedure that allows for a reliable prediction of the top-mass effects using the expansion in $1/m_t$. The quality of the effective field theory to evaluate differential K-factors for the distribution of the hardest jet is found to be better than 1-2% as long as the transverse momentum of the jet is integrated out or remains below about 150 GeV.

DOI: [https://doi.org/10.1007/JHEP11\(2014\)150](https://doi.org/10.1007/JHEP11(2014)150)

Posted at the Zurich Open Repository and Archive, University of Zurich

ZORA URL: <https://doi.org/10.5167/uzh-107555>

Journal Article

Published Version



The following work is licensed under a Creative Commons: Attribution 4.0 International (CC BY 4.0) License.

Originally published at:

Neumann, Tobias; Wiesemann, Marius (2014). Finite top-mass effects in gluon-induced Higgs production with a jet-veto at NNLO. *Journal of High Energy Physics*:150.

DOI: [https://doi.org/10.1007/JHEP11\(2014\)150](https://doi.org/10.1007/JHEP11(2014)150)

RECEIVED: September 2, 2014

ACCEPTED: November 4, 2014

PUBLISHED: November 26, 2014

Finite top-mass effects in gluon-induced Higgs production with a jet-veto at NNLO

Tobias Neumann^a and Marius Wieseemann^b

^a*Fachbereich C, Bergische Universität Wuppertal,
42097 Wuppertal, Germany*

^b*Physik-Institut, Universität Zürich,
8057 Zürich, Switzerland*

E-mail: tobias.neumann@uni-wuppertal.de, marius.wieseemann@cern.ch

ABSTRACT: Effects from a finite top quark mass on the H+ n -jet cross section through gluon fusion are studied for $n = 0/n \geq 1$ at NNLO/NLO QCD. For this purpose, sub-leading terms in $1/m_t$ are calculated. We show that the asymptotic expansion of the jet-vetoed cross section at NNLO is very well behaved and that the heavy-top approximation is valid at the five permille level up to jet-veto cuts of 300 GeV. For the inclusive Higgs+jet rate, we introduce a matching procedure that allows for a reliable prediction of the top-mass effects using the expansion in $1/m_t$. The quality of the effective field theory to evaluate differential K-factors for the distribution of the hardest jet is found to be better than 1–2% as long as the transverse momentum of the jet is integrated out or remains below about 150 GeV.

KEYWORDS: QCD Phenomenology, Jets

ARXIV EPRINT: [1408.6836](https://arxiv.org/abs/1408.6836)

Contents

1	Introduction	1
2	Outline of the calculation	2
3	Results	5
3.1	Input parameters	5
3.2	Notation	5
3.3	Lower order results	6
3.4	Jet-veto at NNLO	9
3.5	Inclusive Higgs+jet rate at NLO	11
3.6	Distributions of the hardest jet	13
4	Conclusions	15
A	Other approximations of the jet-vetoed rate	15
B	Higgs p_T distribution	17

1 Introduction

The discovery of a scalar particle [1, 2] whose properties are compatible with the particle causing the electro-weak symmetry breaking predicted by the Standard Model (SM), i.e. the Higgs boson, was the first observation of a new elementary particle at the Large Hadron Collider (LHC). Initially, the discovery was based on the combination of various experimental search channels. By now, sufficient significance has been reached to claim an observation alone in the two channels $H \rightarrow \gamma\gamma$ [3, 4] and $H \rightarrow ZZ^* \rightarrow 4l$ [3, 5]. Some of the experimental signatures rely heavily on the analysis of particular phase-space regions of the final state particles to reduce the contamination from the background processes. In particular, in the search for $H \rightarrow WW^* \rightarrow l\nu l\nu$ [6, 7] the huge QCD background is reduced using a veto cut ($p_T^{\text{jet}} < p_{T,\text{veto}}^{\text{jet}}$) on jets with a large transverse momentum (p_T). The so-called jet-vetoed cross section is used to lower specifically the $t\bar{t}$ and tW background, where the top quark mainly decays to high- p_T bottom quarks.

In the SM, Higgs production proceeds predominantly through gluon fusion.¹ The jet-vetoed cross section in that case has been known up to NNLO for a while [11]. The residual uncertainties associated with this observable have been subject to recent discussion [12],

¹The gluon fusion process has been studied in great detail over the past years, see refs. [8–10] and references therein.

where the resummation of logarithms in $p_{T,\text{veto}}^{\text{jet}}$ finally allowed to control these uncertainties [13–20]. Another uncertainty, which is very specific to hadronic Higgs production through gluon fusion, is induced by employing an effective theory approach, where the top quark is assumed to be infinitely heavy, to determine higher order corrections to the jet-vetoed rate. Recently, the full top- (m_t) and bottom-mass (m_b) dependence at NLO has been added to the resummed NNLO+NNLL jet-veto efficiencies [21].² At NNLO, finite top-mass effects have been studied in case of the total cross section [25–27] so far, which have been found to be below $\sim 1\%$ [28–32] using an expansion in $1/m_t$ in combination with a matching to the exact result in the limit of large partonic center of mass energies. Differential studies on the validity of the effective field theory approach at this order in the strong coupling constant (α_s) have been considered only for Higgs quantities [33], but not for jet observables.³ They were found to be below 3% as long as the transverse momentum of the Higgs is integrated out or is below ~ 150 GeV.

The goal of this paper is to validate the heavy-top approximation for the Higgs production cross section with a jet-veto at NNLO. For this purpose, we determine the expansion with respect to $1/m_t^k$, where the leading term of this series ($k = 0$) corresponds to the effective field theory. Additionally, we take into account the first and second non-trivial sub-leading term in the $1/m_t^k$ expansion ($k = 2/4$). We supplement our analysis by further jet-related quantities at NLO such as the inclusive one-jet rate and kinematical distributions of the hardest jet. For the jet-vetoed rate, we find that finite top-quark effects for realistic experimental values of the jet-veto cut ($p_{T,\text{veto}}^{\text{jet}} \sim 30$ GeV) are numerically negligible (about five permille). Even for jet-veto cuts up to 600 GeV they remain below two percent. Therefore, we conclude that the use of the effective field theory approach for the jet-vetoed rate is fully justified.

This paper is organized as follows: in section 2, we define the jet-vetoed cross section and set-up the main ingredients of our calculation. Section 3 contains our results, including our default choices of the input parameters, some considerations at lower order and our analysis of finite top-mass effects on the Higgs+ n -jet cross section for $n = 0/n \geq 1$ at NNLO/NLO as well as the NLO p_T and rapidity (y) distribution of the hardest jet. We conclude in section 4.

2 Outline of the calculation

Considering the jet-vetoed (or 0-jet) rate for Higgs production through gluon fusion at NNLO, various contributions have to be taken into account. At LO, the cross section is identical to the total rate, since the only partonic process $gg \rightarrow H$ has no final state jets,⁴ see figure 1 (a). Figure 1 (b) and (c) show two representative purely virtual diagrams to $gg \rightarrow H$ entering at NLO and NNLO, respectively. The partonic processes $gg \rightarrow Hg$,

²Similarly, the full top- and bottom-mass effects on the p_T spectrum of the Higgs at NLO+NLL have been considered in refs. [22–24].

³Further results are only available at leading order (LO) in perturbation theory, for Higgs+ n -jet production with $n = 0, 1, 2$ [34–37].

⁴Since we do not include any parton showering or hadronization, “jet” denotes a cluster of the outgoing partons throughout this paper.

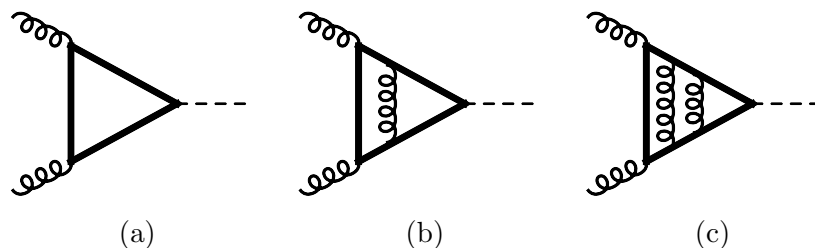


Figure 1. A sample of Feynman diagrams contributing at $p_T = 0$. (a) LO (one-loop); (b) NLO (2-loop); (c) NNLO (3-loop). The graphical notation for the lines is: thick straight $\hat{=}$ top quark; spiraled $\hat{=}$ gluon; dashed $\hat{=}$ Higgs boson.

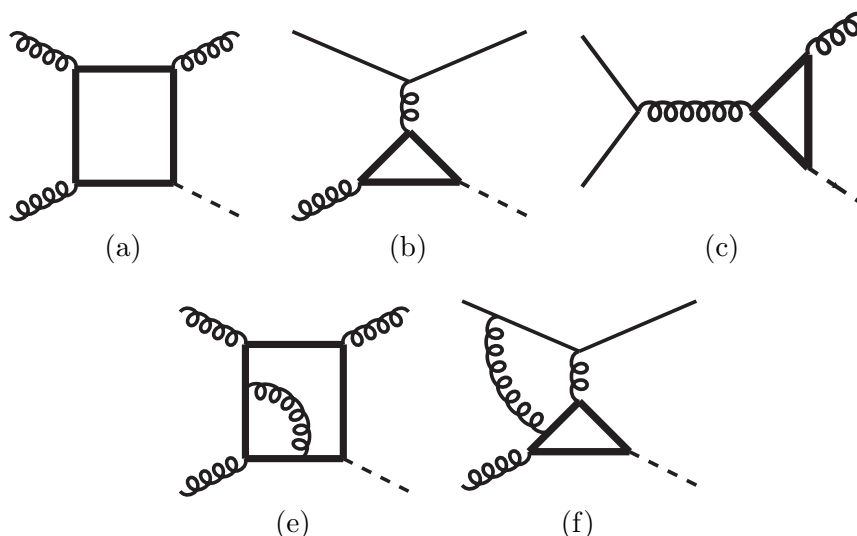


Figure 2. A sample of Feynman diagrams contributing at $p_T > 0$. (a-c) single-real; (e-f) mixed real-virtual. The graphical notation for the lines is: thick straight $\hat{=}$ top quark; thin straight $\hat{=}$ light quark $q \in \{u, d, c, s, b\}$; spiraled $\hat{=}$ gluon; dashed $\hat{=}$ Higgs boson.

$gq \rightarrow Hq$ and $q\bar{q} \rightarrow Hg$ ($q \in \{u, d, s, c, b\}$) at one- and two-loop determine the single real and mixed real-virtual contributions, see figure 2.⁵ Examples for double real emission diagrams are shown in figure 3, the corresponding processes $gg \rightarrow ggH$, $gg \rightarrow q\bar{q}H$, $gq \rightarrow gqH$, $q\bar{q} \rightarrow q\bar{q}H$, $q\bar{q} \rightarrow ggH$, $qq \rightarrow qqH$, $qq' \rightarrow qq'H$ and $\bar{q}q' \rightarrow \bar{q}q'H$ ($q' \neq q$) enter the calculation of the jet-vetoed cross section at NNLO. It is understood that the charge conjugated processes must be included as well.

The most complicated Feynman diagrams are of the two-loop box-type and three-loop-triangle-type with massless and massive (mass m_t) internal and one massive external line (mass m_H),⁶ see figures 2(e) and figures 1(c), for example. Although not out of reach, the complexity of the corresponding integrals is too high for an efficient numerical evaluation. Thus, the NNLO corrections are known only in the effective theory approach with

⁵Note that already the LO process is loop-induced. Thus, the single real emission diagrams contain one loop as well.

⁶ m_H denotes the mass of the Higgs.

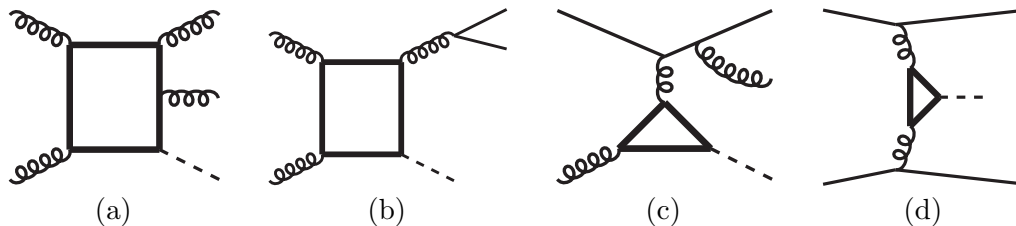


Figure 3. Same as figure 2 but double real emission diagrams.

an infinitely heavy top quark (heavy-top limit). Deploying this approximation the corresponding Feynman diagrams simplify to one and two-loop level without internal masses and with an effective Higgs-gluon vertex, multiplied by a Wilson coefficient which can be evaluated perturbatively [38–42].

In this paper, we go beyond the heavy-top approximation and study the effects of a finite top-quark mass on the jet-vetoed rate. Therefore, we consider the expansion of the cross section with respect to $1/m_t$, whose leading term is given by the effective theory approach. We use the amplitudes which were calculated in ref. [28] by applying automated asymptotic expansions [43–45].

In practice, we obtain the jet-vetoed Higgs cross section by removing all jet contributions $\sigma_{\geq 1\text{-jet}}$ from the total rate σ_{tot} . At NNLO this reads

$$\sigma_{\text{veto}}^{\text{NNLO}} \equiv \sigma_{0\text{-jet}}^{\text{NNLO}} = \sigma_{\text{tot}}^{\text{NNLO}} - \sigma_{\geq 1\text{-jet}}^{\text{NLO}'}, \quad (2.1)$$

where we use the prime-notation of ref. [46] to distinguish $\sigma_{\geq 1\text{-jet}}^{\text{NLO}'}$ calculated with NNLO parton density functions (PDFs) from the proper NLO quantity. For the total rate we deploy the program `ggh@nnlo` [25, 28, 30, 47] including the asymptotic expansion of the amplitudes in $1/m_t^k$ up to $k = 6$.⁷ The calculation of the one-jet inclusive cross section $\sigma_{\geq 1\text{-jet}}$ was carried out using the program described in ref. [33], where we implemented the anti- k_T jet-algorithm [48] to identify QCD jets.⁸ Furthermore, we extended its capabilities to include sub-leading top-mass effects up to $1/m_t^4$. Of course, our setup allows to calculate the exclusive Higgs+ n -jet rates for $n = 1$ and $n = 2$ as well, where we work at NLO and LO accuracy, respectively.

A number of checks have been performed on our results. While the p_T distribution of the Higgs in the heavy-top limit was checked [33] against the fixed order part of the program `HqT` [49–51], we used the program `HNNLO` [24, 52, 53] for a numerical comparison of the jet-vetoed rate. The agreement was found to be better than one percent. At each order in the $1/m_t$ expansion, we explicitly verified the independence of the 0-jet rate with respect to the so-called α -parameter [54, 55], which allows to restrict the phase space of the Catani-Seymour dipoles [56]. The asymptotic expansion of the amplitudes as well as the program `ggh@nnlo` have been validated previously by the agreement of the inclusive cross section between refs. [28] and [31].

⁷We would like to thank Robert Harlander for providing a private version of his code.

⁸Since at most two jets can occur in our calculation, the anti- k_T leads to the same results as the k_T and the Cambridge-Aachen algorithm.

As observed in refs. [30, 32, 33], the $1/m_t$ expansion provides a rather unstable approximation for the purely quark-induced channels, particularly when no matching to the exact result in the high-energy limit is applied. Therefore, these channels constitute a solid, though rather minor limitation of the effective field theory, since their contribution is more than two orders of magnitude smaller than the sum of all channels. We can therefore safely disregard them from our considerations.

3 Results

3.1 Input parameters

We study finite top-mass effects on Higgs+ n -jet cross sections for $n = 0/n \geq 1$ in the gluon fusion process at the LHC with 13 TeV center-of-mass energy. Our choice of the central factorization and renormalization scale is $\mu_F = \mu_R = m_H$, where, if not indicated otherwise $m_H = 125.6$ GeV. All numbers are produced with the MSTW2008 68%CL PDFs [57] which implies that the numerical value for the strong coupling constant is taken as $\alpha_s(m_Z) = 0.13939$ at LO, $\alpha_s(m_Z) = 0.12018$ at NLO, and $\alpha_s(m_Z) = 0.11707$ at NNLO. We set the on-shell top quark mass to $m_t = 173.5$ GeV.

Jets are defined using the anti- k_T algorithm [48] with jet radius: $R = 0.5$. Unless stated otherwise, a jet is required to have transverse momentum of $p_T^{\text{jet}} > 30$ GeV, while we apply no cuts on the Higgs momentum.⁹

3.2 Notation

To deal with the additional expansion of the cross section with respect to $1/m_t$ we introduce the following notation: the truncation of the cross section is defined by

$$[d\sigma^X]_{1/m_t^k}, \quad X \in \{\text{LO, NLO, NNLO}\}, \quad k \in \{0, 2, 4, \dots\} \quad (3.1)$$

where X denotes the order of perturbation theory and k the order at which the $1/m_t^k$ expansion of the cross section is truncated. If the index $1/m_t^k$ and the brackets are absent, it means that the cross section is not truncated and, consequently, $d\sigma^X$ denotes the cross section with exact top-mass dependence. Here and in what follows we imply that all cross sections are reweighted by the exact top-mass dependence at LO:

$$[d\sigma^X]_{1/m_t^k} \equiv [d\bar{\sigma}^X]_{1/m_t^k} \cdot \sigma^{\text{LO}} / [\sigma^{\text{LO}}]_{1/m_t^k}, \quad (3.2)$$

where $d\bar{\sigma}$ denotes the unweighted cross section and σ^{LO} the Born-level cross section for $gg \rightarrow H$.

In order to analyse the perturbative corrections to the cross section, we define the K -factor

$$K_k^X(b) = \frac{[d\bar{\sigma}^X(b)]_{1/m_t^k}}{[d\bar{\sigma}^{\text{LO}}(b)]_{1/m_t^k}}. \quad (3.3)$$

⁹We checked that our results directly generalize to experimentally applied jet definitions for this process which usually imply $p_T^{\text{jet}} > 25\text{-}30$ GeV and a rapidity cut [6, 7].

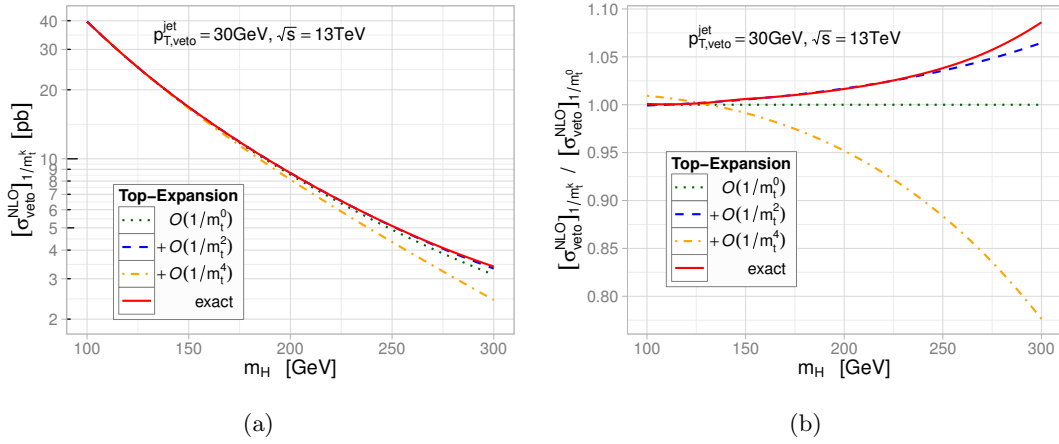


Figure 4. Higgs+0-jet cross section at NLO including terms up to $1/m_t^k$ as a function of m_H for $p_{T,\text{veto}}^{\text{jet}} = 30 \text{ GeV}$. Dotted/dashed/dash-dotted: $k = 0/2/4$. (a) absolute; (b) normalized to $k = 0$.

On the right hand side of this definition, it is understood that $d\sigma(b)$ is integrated over all kinematical variables *except* the set b , where we consider $b = \{p_{T,1}^{\text{jet}}\}$ and $b = \{y_1^{\text{jet}}\}$ (i.e., transverse momentum and rapidity distributions of the hardest jet). For example, $K_0^{\text{NLO}}(p_T^H)$ is the NLO K-factor in the heavy-top limit of the p_T distribution of the Higgs which has been found to be valid at the 2-3% level for $p_T^H \lesssim 150 \text{ GeV}$ [33].¹⁰ Using the $1/m_t$ expansion, we will study whether this observation can be expected to carry over also to jet quantities.

3.3 Lower order results

Figure 4(a) shows the NLO jet-vetoed cross section as a function of the Higgs mass. We applied a veto of $p_{T,\text{veto}}^{\text{jet}} = 30 \text{ GeV}$ on the jet transverse momenta. At this order, the exact dependence on the top-quark mass is known (solid curve).¹¹ Comparing it to the expansion of the cross section up to $1/m_t^k$ for $k = 0$ (dotted curve), $k = 2$ (dashed curve) and $k = 4$ (dash-dotted curve), we can assess the quality of the $1/m_t$ expansion. Clearly, its convergence starts deteriorating once the Higgs mass exceeds the top-quark mass.

In general, the aim of our analysis is to obtain accurate predictions including mass effects for the various jet observable considered in this paper and to use them to estimate the mass corrections with respect to the effective field theory (EFT). The deviation of the higher orders in the asymptotic expansion from the leading term indicates the validity of the EFT to approximate the cross section in the full theory. For this purpose, we normalize all curves to the $1/m_t^0$ approximation in figure 4(b). For small values of m_H , the mass effects are at the percent level. While the expansion up to $1/m_t^2$ remains extremely close to the full result over the whole mass range, the $1/m_t^4$ corrections reduce the cross section significantly towards larger values of m_H . Assuming the exact cross section was

¹⁰Note that in appendix B we extend the analysis of the transverse momentum distribution in ref. [33] by considering an additional term in the $1/m_t^k$ expansion ($k = 4$).

¹¹To obtain the NLO total cross section with exact top-mass dependence we employed the code *SusHi* [58].

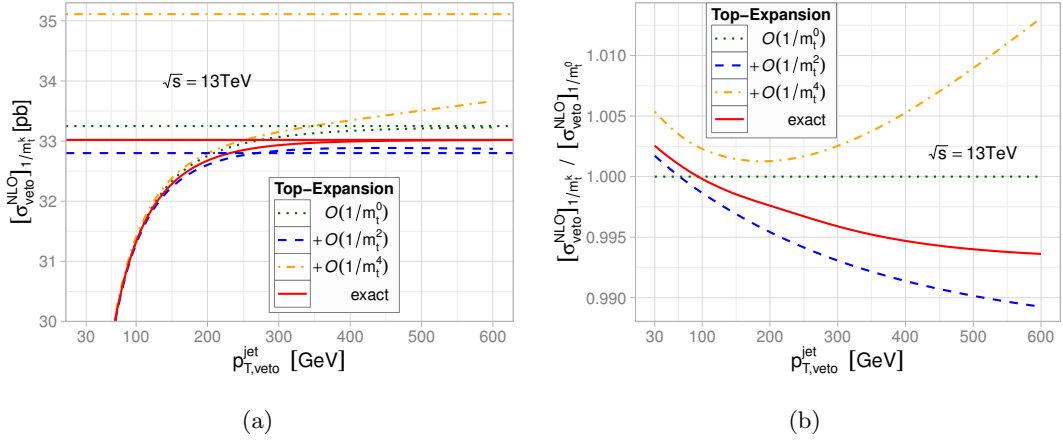


Figure 5. Higgs+0-jet cross section at NLO including terms up to $1/m_t^k$ as a function of $p_{T,veto}^{jet}$. Dotted/dashed/dash-dotted: $k = 0/2/4$. (a) absolute; (b) normalized to $k = 0$.

not known, which is the case at NNLO, we would therefore estimate the uncertainty of the mass corrections on the EFT result to be below 5% for $m_H \lesssim 200$ GeV. Fortunately, all orders of the $1/m_t$ expansion coincide to a very good accuracy at $m_H \simeq 125$ GeV.

In figure 5(a), we study the top-mass corrections to the NLO cross section as a function of the jet-veto cut for $m_H = 125.6$ GeV. The horizontal lines denote the total inclusive cross sections, which correspond to $p_{T,veto}^{jet} \rightarrow \infty$. The agreement between the curves is remarkable. While the differences are at the permille-level for small jet-veto cuts, see figure 5(b), they remain below 2.5% even at $p_{T,veto}^{jet} = 600$ GeV. Again, the asymptotic expansion leads to a proper estimation of the mass effects, not underestimating the uncertainty induced by the heavy-top approximation with respect to exact one. Therefore, the $1/m_t$ terms can be expected to yield a conservative validation of the EFT as well at NNLO.

The reason that the $1/m_t$ expansion of the jet-vetoed rate is well behaved even beyond the $2m_t$ threshold is the phase-space suppression, which strongly reduces contributions from hard jets. However, the $1/m_t^4$ term receives unjustified large contribution from $p_T^{jet} \gtrsim 400$ GeV. In that region, σ_{veto}^{NLO} , $[\sigma_{veto}^{NLO}]_{1/m_t^0}$ as well as $[\sigma_{veto}^{NLO}]_{1/m_t^2}$ develop a flat behavior, which is expected from phase-space suppression, while $[\sigma_{veto}^{NLO}]_{1/m_t^4}$ grows almost linearly. This reveals that the convergence of the amplitudes at $1/m_t^4$ in the large- p_T tail is broken. The previous observations are in direct analogy to the total cross section. In this case, the bulk of the cross section originates from the region $\sqrt{s} \lesssim 2m_t$, in which the asymptotic expansion is well behaved [30]. Nevertheless, the $1/m_t^4$ term receives huge contributions as $\sqrt{s} \gg 2m_t$ [30], since the convergence of the amplitudes is spoiled at large energies. In fact, looking at the total cross sections (horizontal lines) in figure 5(a), it is obvious that the leading and first sub-leading term in the asymptotic expansion compare better to the exact result than when including the $1/m_t^4$ terms.¹²

Turning to the inclusive Higgs+jet cross section, where a cut $p_T^{jet} > p_{T,min}^{jet}$ is applied, which removes the bulk of the well behaved soft jets and, therefore, enhances the contri-

¹²Note that we applied no matching of the total inclusive cross section to the high-energy limit here which will be discussed below.

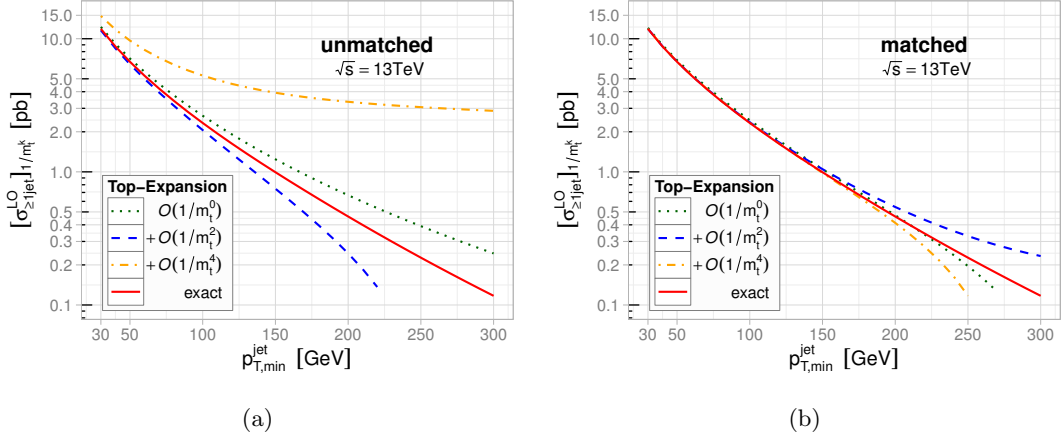


Figure 6. Inclusive Higgs+jet cross section at LO including terms up to $1/m_t^k$ as a function of $p_{T,\min}^{\text{jet}}$. Dotted/dashed/dash-dotted: $k = 0/2/4$. (a) unmatched; (b) matched according to eq. (3.5).

bution from the problematic large- p_T region. Figure 6(a) compares the $1/m_t^k$ expansion of the inclusive Higgs+jet rate at LO for $k = 0/2/4$ to the exact result. While already at $p_{T,\min}^{\text{jet}} = 30$ GeV the deviation between the curves relative to $1/m_t^0$ is quite large ($\sim 27\%$), convergence of the asymptotic expansion is completely lost at large values of $p_{T,\min}^{\text{jet}}$. Thus, we cannot use the ordinary $1/m_t$ expansion to determine a sensible estimate of the mass effects on the inclusive Higgs+jet rate.

However, the same problematic effects contribute to the total inclusive cross section σ_{tot} , as we have seen before. In this case, a matching to the high-energy limit was performed as described in ref. [30] to control the region $\sqrt{s} > 2m_t$. Similarly, a matching of the inclusive Higgs+jet cross section to the $p_T \rightarrow \infty$ limit would temper unjustified effects from high- p_T jets. Let us assume this matched cross section was known and call it $\sigma_{\geq 1\text{-jet, matched}}$. Given the fact that the total cross section can be viewed as the integral over the p_T distribution and the asymptotic expansion in the small- p_T region works almost perfectly, the following relation should be valid up to a very good precision as long as $p_{T,\min}^{\text{jet}}$ remains at moderate values:¹³

$$[\sigma_{\text{tot, matched}}^{\text{NLO}}]_{m_t^k} - [\sigma_{\text{tot, unmatched}}^{\text{NLO}}]_{m_t^k} = [\sigma_{\geq 1\text{-jet, matched}}^{\text{LO}'}]_{m_t^k} - [\sigma_{\geq 1\text{-jet, unmatched}}^{\text{LO}'}]_{m_t^k}, \quad (3.4)$$

where the primed LO quantity is calculated with NLO parton distributions, as defined in section 2. This equation allows us to determine the matched inclusive Higgs+jet cross section by using LO PDFs for all quantities:

$$[\sigma_{\geq 1\text{-jet, matched}}^{\text{LO}}]_{m_t^k} \equiv [\sigma_{\geq 1\text{-jet, unmatched}}^{\text{LO}}]_{m_t^k} + [\sigma_{\text{tot, matched}}^{\text{NLO}*}]_{m_t^k} - [\sigma_{\text{tot, unmatched}}^{\text{NLO}*}]_{m_t^k}, \quad (3.5)$$

where we defined the starred NLO cross section to be evaluated with LO PDFs. Figure 6(b) shows the matched cross section as defined in eq. (3.5). It is very impressive how close all curves are to the exact result with respect to the unmatched case in figure 6(a).

¹³With “moderate values” we mean values at which the asymptotic expansion works well. The usual jet definitions with $p_{T,\min}^{\text{jet}} \sim 30$ GeV are well within that region.

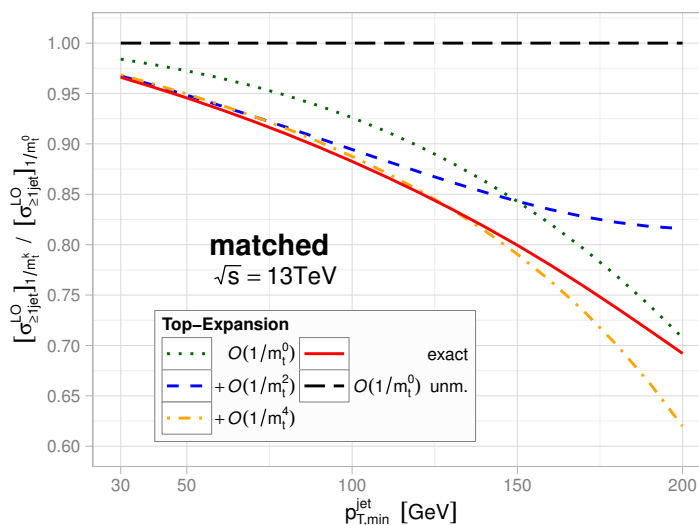


Figure 7. Same as figure 6(b), but normalized to the unmatched $1/m_t^0$ cross section (dotted curve of figure 6(a)).

In figure 7, the matched predictions of figure 6(b) are normalized to the unmatched cross section in the heavy-top limit (dotted curve in figure 6(a)). Comparing first the matched cross sections to the exact curve, their overall agreement is remarkable ($\lesssim 5\%$ for $p_{T,\min}^{\text{jet}} \leq 150$ GeV). In that region, they are successively closer to the exact result, as k increases. The deviation of the EFT result from the matched curves on the other hand allows its validation at the 3 – 10% level for $p_{T,\text{veto}}^{\text{jet}} \in [30, 100]$ GeV. Thus, with the definition of the matched cross section we not only recovered the ability to validate the heavy-top limit for the inclusive Higgs+jet rate, we also found a way to reliably predict the cross section for moderate $p_T^{\min} \lesssim 100$ GeV. This will prove useful at NLO, where the exact result is not available.

There are cases in our analysis where the reliability of the $1/m_t$ expansion appears to be exceptionally good. This happens when the $1/m_t^4$ corrections become negligible and, consequently, the expansions up to $1/m_t^2$ and up to $1/m_t^4$ almost coincide. We already observed this twice: in figure 4(b) around $m_H = 125$ GeV and in figure 7 for $p_{T,\text{veto}}^{\text{jet}} \lesssim 90$ GeV. In both cases, the dashed curve (contributions up to $1/m_t^2$) and the dash-dotted curve (contributions up to $1/m_t^4$) are basically on top of each other and approximate the exact result extremely well ($< 1\%$).

Overall, our observations so far are encouraging to study the behavior of the $1/m_t$ expansion at higher orders to estimate the range of applicability of the heavy-top limit for jet observables.

3.4 Jet-veto at NNLO

We are now ready to analyze the mass effects on the jet-vetoed rate at NNLO, which is the central observable of our study. Figure 8(a) shows the truncation of the cross section with a jet-veto at $1/m_t^k$ for $k = 0$ (dotted), $k = 2$ (dashed) and $k = 4$ (dash-

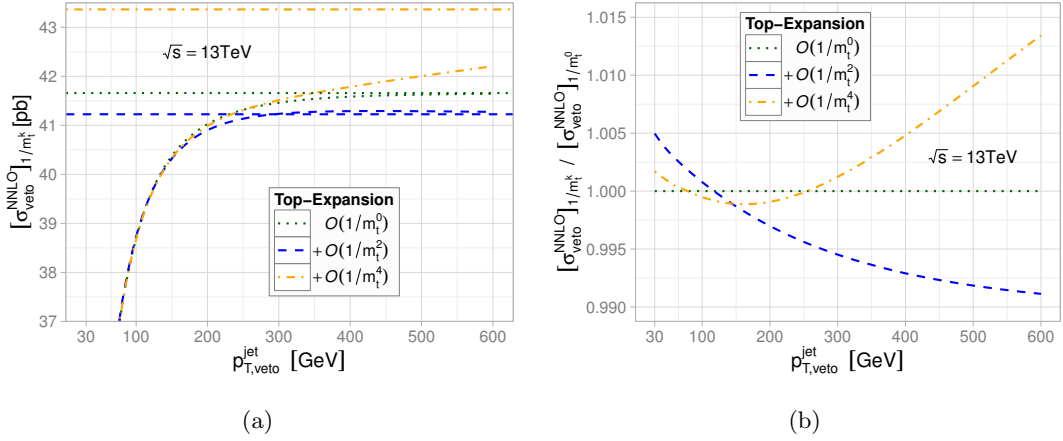


Figure 8. Higgs+0-jet cross section at NNLO including terms up to $1/m_t^k$ as a function of $p_{T,veto}^{jet}$. Dotted/dashed/dash-dotted: $k = 0/2/4$. (a) absolute; for reference, the horizontal lines display the corresponding total cross sections in the three approximations; (b) normalized to $k = 0$.

dotted) as a function of the jet-veto cut. At small values of $p_{T,veto}^{jet}$, we observe an excellent convergence of the asymptotic expansion, i.e. the cross section is almost independent of the order of expansion in $1/m_t$. For example, the spread of the curves is about 0.5% at $p_{T,veto}^{jet} = 30$ GeV, see figure 8(b), where all curves are normalized to the EFT ($k = 0$). In fact, $[\sigma_{veto}^{NNLO}]_{1/m_t^k}$ behaves even better with increasing k than the total inclusive cross section, where a matching to the high-energy limit is required [30] to alleviate the unjustified large effects from hard jets. These effects do not appear in case of the jet-vetoed cross section. More precisely, they explicitly cancel between σ_{tot}^{NNLO} and $\sigma_{\geq 1-jet}^{NLO'}$ in eq. (2.1).

At larger values of the jet-veto cut, the deviation between the curves in figure 8 increases. It stays remarkably small though ($\sim 2\%$ at $p_{T,veto}^{jet} = 600$ GeV). Thus, similarly to what we found at NLO, the asymptotic expansion of the cross section is well behaved even for a jet-veto cut beyond the $2m_t$ threshold, because contributions from large- p_T jets are suppressed by phase-space.¹⁴

In a large number of beyond standard model (BSM) theories, additional scalar particles are predicted, e.g. a second (heavier) CP-even Higgs boson. Therefore, we investigate the quality of the $m_t \rightarrow \infty$ approximation for more general Higgs masses. Figure 9 shows the $1/m_t^k$ expansion ($k = 0/2/4$) of the jet-vetoed NNLO cross section normalized to the EFT result ($k = 0$) as a function of m_H . Indeed, the effective field theory yields a valid approximation at the one-percent level for $m_H \lesssim 150$ GeV. At larger Higgs masses the top-mass effects become sizable and the uncertainty induced by the heavy-top limit increases to ~ 6 (25)% at $m_H = 200$ (300) GeV.

In summary, for a SM Higgs boson of mass 125.6 GeV it is fully justified to trust the effective field theory approach to determine radiative corrections to the jet-vetoed cross section at NNLO. It is advisable, though, to account for the full mass dependence at LO through reweighting, as it is common practice and done in our analysis.¹⁵ Further-

¹⁴As we see in section 3.6, mass effects become important once the transverse momenta of the hardest jet exceeds ~ 150 GeV.

¹⁵In appendix A the mass effects on the corresponding cross section reweighted with the full NLO mass

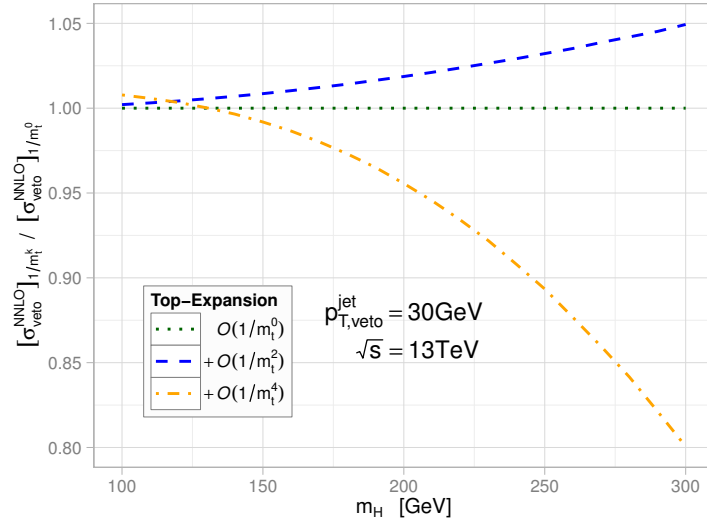


Figure 9. Higgs+0-jet cross section at NNLO including terms up to $1/m_t^k$ as a function of m_H normalized to heavy-top limit ($k = 0$) for $p_{T,\text{veto}}^{\text{jet}} = 30$ GeV. Dotted/dashed/dash-dotted: $k = 0/2/4$.

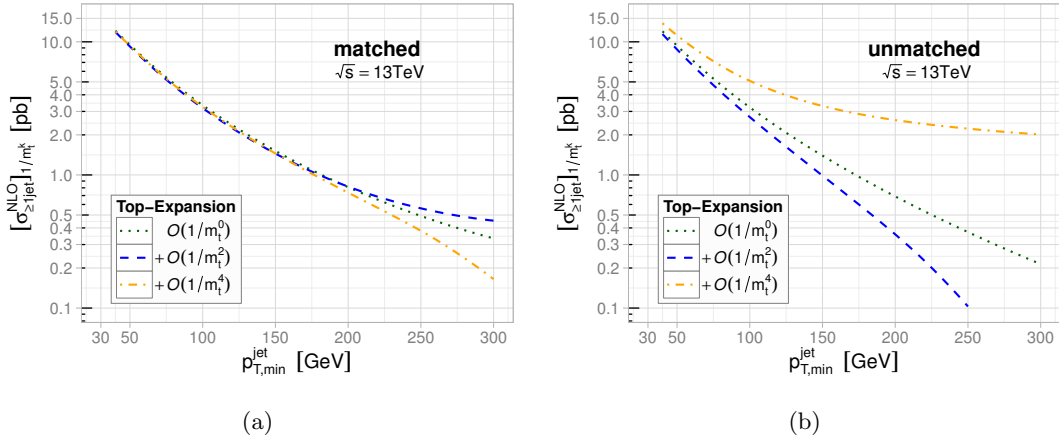


Figure 10. Inclusive Higgs+jet cross section at NLO including terms up to $1/m_t^k$ as a function of $p_{T,\text{min}}^{\text{jet}}$. Dotted/dashed/dash-dotted: $k = 0/2/4$. (a) matched according to eq. (3.6); (b) unmatched.

more, our results should directly generalize to the resummed jet-vetoed cross section at NNLO+NNLL [16] evaluated in the EFT, since the resummation of Sudakov logarithms from soft-gluon emissions is predominantly described by process independent QCD effects.

3.5 Inclusive Higgs+jet rate at NLO

For the LO Higgs+jet cross section, the $1/m_t$ expansion provides no proper approximation of the top-mass effects, as we have seen in section 3.3. The reason for this are unjustified large contributions from high- p_T jets at higher orders in $1/m_t$. In order to obtain a reliable

dependence are studied. We find very similar results in this case.

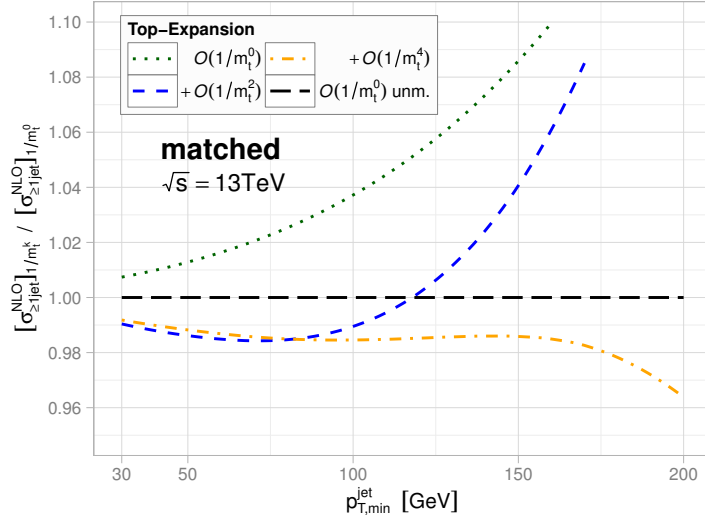


Figure 11. Same as figure 10(a), but normalized to the unmatched $1/m_t^0$ cross section (dotted curve of figure 10(b)).

estimate of the mass effects on the LO Higgs+jet rate, we defined the matched cross section in eq. (3.5). Moving to α_s^4 , we encounter the same problems, which can be seen from the dash-dotted curve (expansion up to $1/m_t^4$) in figure 8(a) at $p_T^{\text{jet}} \gtrsim 400$ GeV, for example. Consequently, not only the LO Higgs+jet cross section is affected, but also the NLO one. This is why we define the matched inclusive Higgs+jet rate at NLO accordingly:

$$[\sigma_{\geq 1\text{-jet}}^{\text{NLO}}]_{m_t^k}^{\text{matched}} \equiv [\sigma_{\geq 1\text{-jet}}^{\text{NLO}}]_{m_t^k}^{\text{unmatched}} + [\sigma_{\text{tot}}^{\text{NNLO}^*}]_{m_t^k}^{\text{matched}} - [\sigma_{\text{tot}}^{\text{NNLO}^*}]_{m_t^k}^{\text{unmatched}}, \quad (3.6)$$

where the starred NNLO cross section is calculated with NLO PDFs.

The matched cross section expanded up to different orders in $1/m_t^k$ is shown in figure 10(a) ($k = 0/2/4$). All three curves are very close, extending the validity of the asymptotic expansion to significantly larger values of $p_{T,\text{min}}^{\text{jet}}$ than in the unmatched case, see figure 10(b). Figure 11 shows the improved matched predictions of figure 10(a) normalized to the unmatched cross section in the heavy-top limit (dotted curve of figure 10(b)). The $1/m_t^4$ term yields a very small correction for $p_{T,\text{min}}^{\text{jet}} \in [30, 100]$ GeV. In this case, we trust the dashed (expansion up to $1/m_t^2$) and dashed-dotted curve (expansion up to $1/m_t^4$) to approximate the exact mass effects to better than one percent. Therefore, as long as the minimum jet- p_T cut remains at moderate values ($p_{T,\text{min}}^{\text{jet}} \lesssim 100$ GeV) the definition of the matched cross section in eq. (3.5) and eq. (3.6) allows us to determine a reliable prediction of the inclusive Higgs+jet rate at LO and NLO, respectively. Furthermore, comparing the matched curve at $1/m_t^4$ to the unmatched EFT result, we validate the heavy-top approximation at the level of 1-2% for $p_{T,\text{min}}^{\text{jet}} \leq 100$ GeV.

This result shows that the EFT, in fact, works better in the problematic high- p_T region than the corresponding sub-leading $1/m_t$ terms, which are far apart in the unmatched case, see figure 10(b). This is very similar to what was found for the total cross section [30], where it was argued that in the heavy-top limit ($k = 0$) problematic terms $(\sqrt{s}/m_t)^k$ vanish,

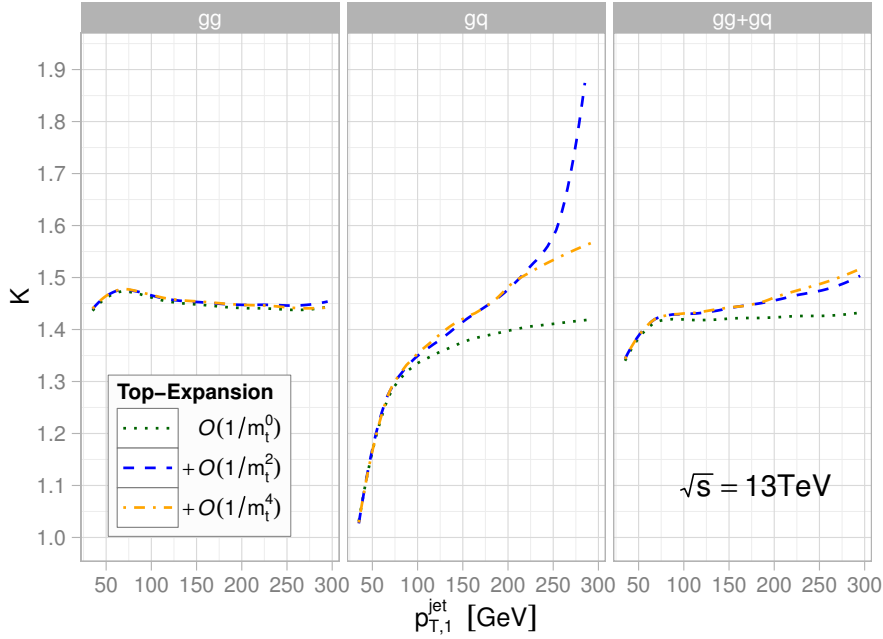


Figure 12. K -factors as defined in eq. (3.3), for the transverse momentum distribution of the hardest jet, i.e. $K_k^{\text{NLO}} \equiv K_k^{\text{NLO}}(p_{T,1}^{\text{jet}})$. Left/center/right plot: only gg /only qg /sum of gg and qg . Dotted/dashed/dash-dotted: $k = 0/2/4$.

which spoil the convergence of the asymptotic expansion ($k > 0$) in the high-energy region. Also in this case the matching to the high-energy limit revealed that the unmatched EFT result is valid at the percent level.

However, at larger values ($p_{T,\text{min}}^{\text{jet}} > 100 \text{ GeV}$), the asymptotic expansion starts deteriorating significantly also for the matched cross section in figure 11. Therefore, the uncertainty of the EFT due to mass effects in that region is quite sizable. For comparison, the deviation of the EFT from the exact curve is 12(30)% for $p_{T,\text{min}}^{\text{jet}} = 100(200) \text{ GeV}$ at LO, see figure 7.

3.6 Distributions of the hardest jet

Finally, let us consider kinematical distributions of the hardest jet. Figure 12 shows the p_T -dependent K -factors $K_k^{\text{NLO}} \equiv K_k^{\text{NLO}}(p_{T,1}^{\text{jet}})$ of the cross section up to $1/m_t^k$ as defined in eq. (3.3) with variable scales

$$\mu_F = \mu_R = \sqrt{m_H^2 + (p_{T,1}^{\text{jet}})^2}. \quad (3.7)$$

In the gg -channel, all three K -factors are almost identical. However, the QCD corrections to the subleading mass terms in the qg -channel behave quite differently to the EFT result once $p_{T,1}^{\text{jet}} \gtrsim 100 \text{ GeV}$. In the sum of both channels though, the difference remains below $\sim 1.5\%$ for $p_{T,1}^{\text{jet}} < 150 \text{ GeV}$, and reaches 6% at $p_{T,1}^{\text{jet}} = 300 \text{ GeV}$. Therefore, our results turn out to be quite similar to what was already found for the p_T distribution of the Higgs $K_k^{\text{NLO}}(p_T^H)$ [33], yet the asymptotic behavior is slightly improved for the hardest jet. For

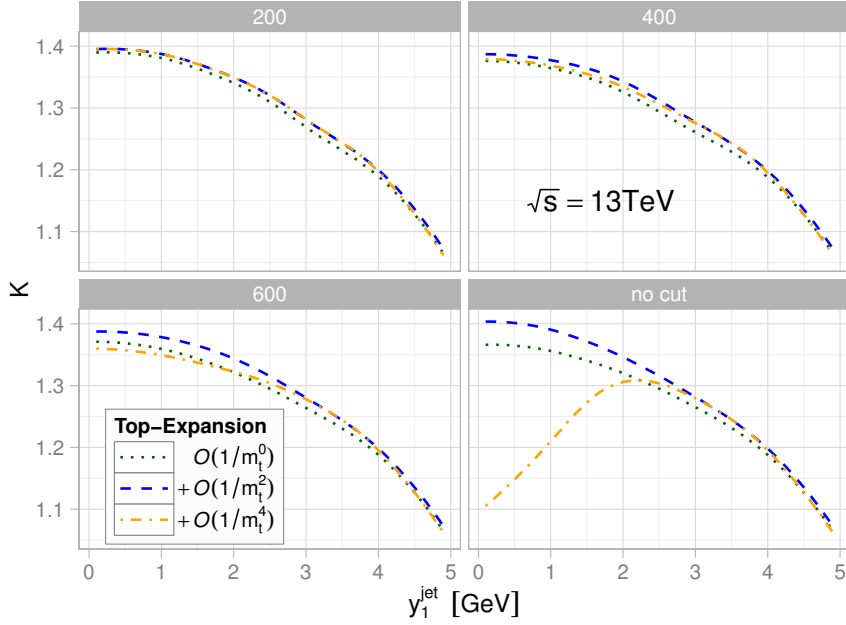


Figure 13. K -factors as defined in eq. (3.3), for the rapidity distribution of the hardest jet, i.e. $K_k^{\text{NLO}} \equiv K_k^{\text{NLO}}(y_1^{\text{jet}})$. Left-top/right-top/left-bottom/right-bottom plot: $p_{T,\max}^{\text{jet}} = 200$ GeV/400 GeV/600 GeV/no cut. Dotted/dashed/dash-dotted: $k = 0/2/4$.

comparison, we give an updated result for $K_k^{\text{NLO}}(p_T^H)$ up to $1/m_t^4$ in appendix B, which shows that K_4^{NLO} behaves quite differently in the two cases at high p_T .

Note that the $1/m_t^4$ corrections are extremely small for $p_{T,1}^{\text{jet}} \lesssim 200$ GeV in figure 12. We conclude therefore that the quality of K_2^{NLO} and K_4^{NLO} to approximate the exact top-mass effects is better than one percent in that region.

The situation for the rapidity distribution of the hardest jet is more involved. The problem is that in the central region the $1/m_t^4$ term receives unjustified large effects from hard jets, which spoil the convergence of the asymptotic series. Unfortunately, it is not possible to determine a matched cross section in this case, similarly to what we do for the inclusive Higgs+jet cross section. Instead, we introduce a cut $p_T^{\text{jet}} < p_{T,\max}^{\text{jet}}$ which simply removes the problematic high- p_T jets. This cut is of course arbitrary, therefore, we choose three different values: $p_{T,\max}^{\text{jet}} = 200, 400, 600$ GeV.

The contribution to the y_1^{jet} distribution from jets with $p_T^{\text{jet}} > 600$ GeV should be completely negligible due to phase-space suppression. Indeed, this is what we observe for the EFT result, but not for the subleading terms in the $1/m_t$ expansion, see figure 13, which shows $K_k^{\text{NLO}} \equiv K_k^{\text{NLO}}(y_1^{\text{jet}})$ for $p_{T,\max}^{\text{jet}} = 200, 400, 600$ GeV and without cut. Clearly, the asymptotic behavior in the central region is broken without a cut. It works pretty well though once we apply an upper cut on the jets. The EFT result is almost identical ($< 0.5\%$) in the lower two plots and receives no unjustified large effects from high- p_T jets. Therefore, it is legitimate to estimate the quality of the EFT without a cut from the results for $p_{T,\max}^{\text{jet}} = 600$ GeV, which we deduce to be better than 2% in the central region and even below one percent in the forward region ($y_1^{\text{jet}} > 2.5$).

In conclusion, the behavior of the K -factors of the hardest jet distributions suggests that the QCD corrections can be safely calculated in the heavy-top approximation. The accuracy remains within 1.5% (6%) below $p_{T,1}^{\text{jet}} = 150 \text{ GeV}$ ($p_{T,1}^{\text{jet}} = 300 \text{ GeV}$) and for p_T -integrated quantities at the percent level.

4 Conclusions

Finite top-mass effects in the gluon fusion process have been studied. The quality of the effective field theory to describe the exact cross section was estimated using subleading terms in $1/m_t$. They have been evaluated for various jet quantities, namely, the NNLO cross section with a jet veto, the inclusive Higgs+jet rate at NLO and the NLO K -factors of jet distributions.

The corrections of a finite top-mass to the jet-vetoed rate are negligible and the quality of the effective field theory to describe this quantity even at large values of the jet-veto cut is remarkable. Unjustified large contribution from hard jets were found to spoil the convergence of the asymptotic expansion in case of the inclusive Higgs+jet cross section. Only a matching procedure involving the total inclusive cross section allowed for a reliable prediction of this quantity and the estimation of the mass effects from the $1/m_t$ expansion. The EFT was then found to be valid even without the matching at the 1-2% level for jet definitions with a minimal transverse momentum cut lower than 100 GeV. For large values of the jet p_T cut though, the asymptotic expansion of the matched result becomes unreliable. Therefore, also the uncertainty induced by the EFT is large, deviating by 30% from the exact result already at LO for a minimal jet cut of 200 GeV.

Also the perturbative corrections to distributions of the hardest jet turned out to have a rather mild top-mass dependence. For the transverse momentum distribution, the procedure of correcting the LO prediction including the exact top-mass dependence by the K -factor evaluated in the EFT provides an excellent approximation to the full NLO result, valid to better than 1.5(6)% for $p_T^{\text{jet}} < 150(300) \text{ GeV}$. The K -factor of the rapidity distribution determined in the heavy-top limit was validated at the 1-2% level.

We have checked that our results hold also for different machine energies at the LHC. The accuracy of the effective field theory approach is better than the uncertainty on the cross section induced by the PDFs and missing higher order QCD corrections.

Acknowledgments

We would like to thank Pier Francesco Monni for useful comments on the manuscript. We are indebted to Robert Harlander for fruitful discussions, his comments on the manuscript and the private version of his code `ggh@nnlo` that he provided for our study. The work of TN was supported by BMBF contract 05H12PXE. MW was supported by the European Commission through the FP7 Marie Curie Initial Training Network “LHCPhenoNet” (PITN-GA-2010-264564).

A Other approximations of the jet-vetoed rate

Since the exact top-mass dependence on the jet-vetoed rate is unknown at NNLO, various approximations can be employed for the cross section prediction. In section 3.4 we apply

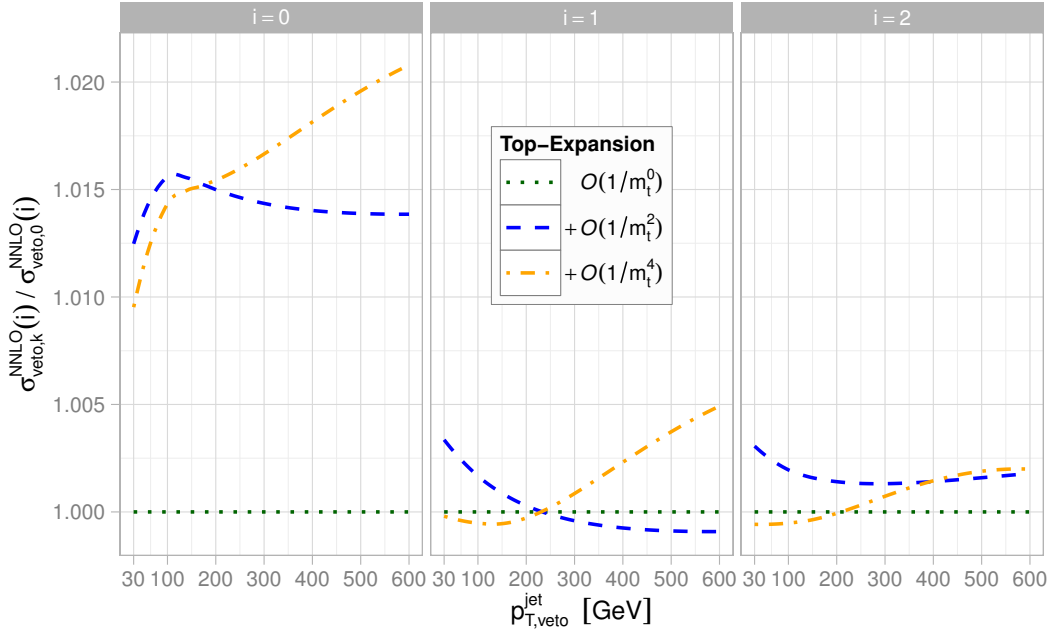


Figure 14. Same as figure 8(b), but for the approximations defined in eq. (A.1). Left/center/right plot show the ratios $R_k(0)/R_k(1)/R_k(2)$ defined in eq. (A.3).

the effective field theory and account for the exact top-mass effects at LO by the means of reweighting. This method corresponds to calculating radiative corrections, namely the K -factor from LO to NNLO, in the effective field theory and multiplying it with the LO cross section in the full theory. However, the full top-mass dependence is known through NLO and therefore, we may employ it to determine the jet-vetoed rate at NNLO.¹⁶

In this appendix we consider the following approximations of the jet-vetoed rate at NNLO:

$$\sigma_{\text{veto},k}^{\text{NNLO}}(i) \equiv \sigma_{\text{veto}}^{\text{NLO}'} + \kappa_i \cdot \left([\sigma_{\text{veto}}^{\text{NNLO}}]_{1/m_t^k} - [\sigma_{\text{veto}}^{\text{NLO}'}]_{1/m_t^k} \right), \quad (\text{A.1})$$

where

$$\kappa_0 = 1, \quad \kappa_1 = \sigma_{\text{veto}}^{\text{LO}} / [\sigma_{\text{veto}}^{\text{LO}}]_{1/m_t^k} = \sigma^{\text{LO}} / [\sigma^{\text{LO}}]_{1/m_t^k}, \quad \kappa_2 = \sigma_{\text{veto}}^{\text{NLO}'} / [\sigma_{\text{veto}}^{\text{NLO}'}]_{1/m_t^k}. \quad (\text{A.2})$$

In fact, using κ_2 in eq. (A.1) corresponds to calculating the K -factor from NLO to NNLO in the effective field theory and multiplying it with the NLO cross section in the full theory.

In figure 14, we study the mass effects on the jet-vetoed cross section in the various approximations ($i = 0, 1, 2$) of eq. (A.1) by considering the ratio

$$R_k(i) = \sigma_{\text{veto},k}^{\text{NNLO}}(i) / \sigma_{\text{veto},0}^{\text{NNLO}}(i). \quad (\text{A.3})$$

¹⁶We thank the referee for this suggestion.

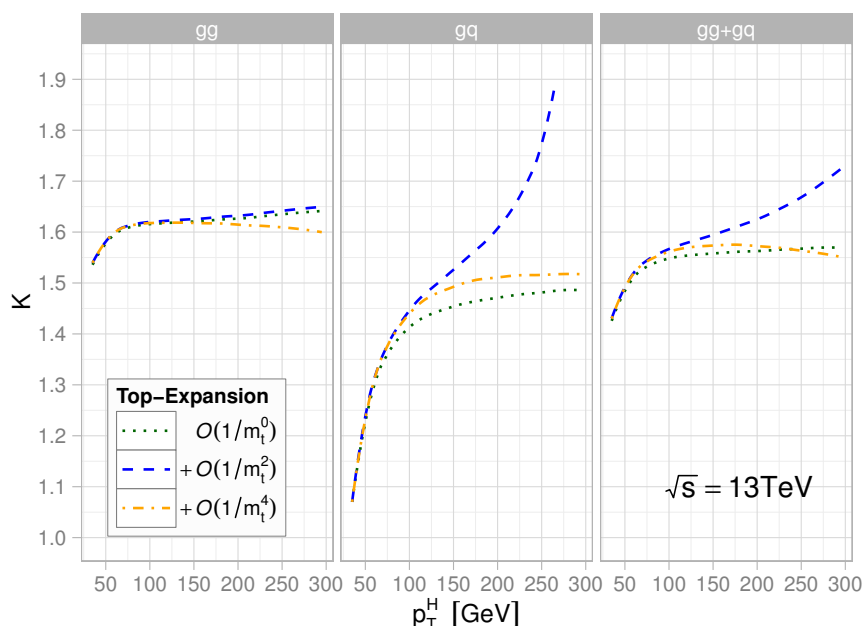


Figure 15. Same as figure 12, but for the transverse momentum distribution of the Higgs; here: $K_k^{\text{NLO}} \equiv K_k^{\text{NLO}}(p_T^H)$.

These plots correspond to figure 8(b), where we used the LO-reweighted effective field theory result for the jet-vetoed cross section. Clearly, in terms of mass effects the approximation used in the left plot ($i = 0$) is considerably worse than the other two. The mass effects are at the level of 1-2% in this case. This is expected, since in general the heavy-top limit works better to describe radiative corrections than the absolute cross section, which is used for the NNLO contribution in the κ_0 -approximation. This is substantiated by the fact that applying the same procedure at NLO the mass effects turn out to be larger as well.

Considering the κ_1 - and κ_2 -approximation in figure 14, i.e., the center and right plot, respectively, the conclusions are very similar to what has been found in section 3.4: the mass effects are extremely small ($< 0.5\%$) for jet-veto cuts up to 600 GeV. Actually, the behavior is even slightly better than for our default approximation in figure 8(b), which stems from fact that in the approach at hand the full cross section is taken into account up to the NLO.

Finally, we checked that the absolute values of the jet-vetoed cross section in the various approaches considered in this paper at NNLO differ by less than 1%, once mass effects are correctly accounted for.

B Higgs p_T distribution

For completeness, we update the results of ref. [33] for the K -factors of the transverse momentum distribution of the Higgs $K_k^{\text{NLO}}(p_T^H)$, see figure 15. The factorization and renormalization scale are set to the transverse mass of the Higgs

$$\mu_F = \mu_R = m_T^H = \sqrt{m_H^2 + (p_T^H)^2}. \quad (\text{B.1})$$

Additionally to ref. [33], we determine the K -factor expanded up to $1/m_t^4$. Our result perfectly confirms the conclusions drawn in that paper, since K_4 lies just right between K_0 and K_2 for most transverse momenta.

Open Access. This article is distributed under the terms of the Creative Commons Attribution License ([CC-BY 4.0](https://creativecommons.org/licenses/by/4.0/)), which permits any use, distribution and reproduction in any medium, provided the original author(s) and source are credited.

References

- [1] ATLAS collaboration, *Observation of a new particle in the search for the standard model Higgs boson with the ATLAS detector at the LHC*, *Phys. Lett. B* **716** (2012) 1 [[arXiv:1207.7214](https://arxiv.org/abs/1207.7214)] [[INSPIRE](#)].
- [2] CMS collaboration, *Observation of a new boson at a mass of 125 GeV with the CMS experiment at the LHC*, *Phys. Lett. B* **716** (2012) 30 [[arXiv:1207.7235](https://arxiv.org/abs/1207.7235)] [[INSPIRE](#)].
- [3] ATLAS collaboration, *Measurements of Higgs boson production and couplings in diboson final states with the ATLAS detector at the LHC*, *Phys. Lett. B* **726** (2013) 88 [[arXiv:1307.1427](https://arxiv.org/abs/1307.1427)] [[INSPIRE](#)].
- [4] CMS collaboration, *Observation of the diphoton decay of the Higgs boson and measurement of its properties*, *Eur. Phys. J. C* **74** (2014) 3076 [[arXiv:1407.0558](https://arxiv.org/abs/1407.0558)] [[INSPIRE](#)].
- [5] CMS collaboration, *Measurement of the properties of a Higgs boson in the four-lepton final state*, *Phys. Rev. D* **89** (2014) 092007 [[arXiv:1312.5353](https://arxiv.org/abs/1312.5353)] [[INSPIRE](#)].
- [6] ATLAS collaboration, *Search for the Higgs boson in the $H \rightarrow WW \rightarrow l\nu jj$ decay channel at $\sqrt{s} = 7$ TeV with the ATLAS detector*, *Phys. Lett. B* **718** (2012) 391 [[arXiv:1206.6074](https://arxiv.org/abs/1206.6074)] [[INSPIRE](#)].
- [7] CMS collaboration, *Measurement of Higgs boson production and properties in the WW decay channel with leptonic final states*, *JHEP* **01** (2014) 096.
- [8] LHC HIGGS CROSS SECTION WORKING GROUP collaboration, S. Dittmaier et al., *Handbook of LHC Higgs cross sections: 1. Inclusive observables*, [arXiv:1101.0593](https://arxiv.org/abs/1101.0593) [[INSPIRE](#)].
- [9] LHC HIGGS CROSS SECTION WORKING GROUP collaboration, S. Dittmaier et al., *Handbook of LHC Higgs cross sections: 2. Differential distributions*, [arXiv:1201.3084](https://arxiv.org/abs/1201.3084) [[INSPIRE](#)].
- [10] LHC HIGGS CROSS SECTION WORKING GROUP collaboration, S. Heinemeyer et al., *Handbook of LHC Higgs cross sections: 3. Higgs properties*, [arXiv:1307.1347](https://arxiv.org/abs/1307.1347) [[INSPIRE](#)].
- [11] S. Catani, D. de Florian and M. Grazzini, *Direct Higgs production and jet veto at the Tevatron and the LHC in NNLO QCD*, *JHEP* **01** (2002) 015 [[hep-ph/0111164](https://arxiv.org/abs/hep-ph/0111164)] [[INSPIRE](#)].
- [12] I.W. Stewart and F.J. Tackmann, *Theory uncertainties for Higgs and other searches using jet bins*, *Phys. Rev. D* **85** (2012) 034011 [[arXiv:1107.2117](https://arxiv.org/abs/1107.2117)] [[INSPIRE](#)].
- [13] C.F. Berger et al., *Higgs production with a central jet veto at NNLL + NNLO*, *JHEP* **04** (2011) 092.
- [14] A. Banfi, G.P. Salam and G. Zanderighi, *NLL+NNLO predictions for jet-veto efficiencies in Higgs-boson and Drell-Yan production*, *JHEP* **06** (2012) 159 [[arXiv:1203.5773](https://arxiv.org/abs/1203.5773)] [[INSPIRE](#)].
- [15] F.J. Tackmann, J.R. Walsh and S. Zuberi, *Resummation properties of jet vetoes at the LHC*, *Phys. Rev. D* **86** (2012) 053011 [[arXiv:1206.4312](https://arxiv.org/abs/1206.4312)] [[INSPIRE](#)].

- [16] A. Banfi, P.F. Monni, G.P. Salam and G. Zanderighi, *Higgs and Z-boson production with a jet veto*, *Phys. Rev. Lett.* **109** (2012) 202001 [[arXiv:1206.4998](#)] [[INSPIRE](#)].
- [17] T. Becher and M. Neubert, *Factorization and NNLL resummation for Higgs production with a jet veto*, *JHEP* **07** (2012) 108 [[arXiv:1205.3806](#)] [[INSPIRE](#)].
- [18] X. Liu and F. Petriello, *Resummation of jet-veto logarithms in hadronic processes containing jets*, *Phys. Rev. D* **87** (2013) 014018 [[arXiv:1210.1906](#)] [[INSPIRE](#)].
- [19] T. Becher, M. Neubert and L. Rothen, *Factorization and N^3LL_p +NNLO predictions for the Higgs cross section with a jet veto*, *JHEP* **10** (2013) 125 [[arXiv:1307.0025](#)] [[INSPIRE](#)].
- [20] I.W. Stewart, F.J. Tackmann, J.R. Walsh and S. Zuberi, *Jet p_T resummation in Higgs production at NNLL' + NNLO*, *Phys. Rev. D* **89** (2014) 054001 [[arXiv:1307.1808](#)] [[INSPIRE](#)].
- [21] A. Banfi, P.F. Monni, G. Zanderighi, *Quark masses in Higgs production with a jet veto*, *JHEP* **01** (2014) 097 [[arXiv:1308.4634](#)] [[INSPIRE](#)].
- [22] E. Bagnaschi, G. Degrossi, P. Slavich and A. Vicini, *Higgs production via gluon fusion in the POWHEG approach in the SM and in the MSSM*, *JHEP* **02** (2012) 088 [[arXiv:1111.2854](#)] [[INSPIRE](#)].
- [23] H. Mantler and M. Wiesemann, *Top- and bottom-mass effects in hadronic Higgs production at small transverse momenta through LO+NLL*, *Eur. Phys. J. C* **73** (2013) 2467 [[arXiv:1210.8263](#)] [[INSPIRE](#)].
- [24] M. Grazzini and H. Sargsyan, *Heavy-quark mass effects in Higgs boson production at the LHC*, *JHEP* **09** (2013) 129 [[arXiv:1306.4581](#)] [[INSPIRE](#)].
- [25] R.V. Harlander and W.B. Kilgore, *Next-to-next-to-leading order Higgs production at hadron colliders*, *Phys. Rev. Lett.* **88** (2002) 201801 [[hep-ph/0201206](#)] [[INSPIRE](#)].
- [26] C. Anastasiou and K. Melnikov, *Higgs boson production at hadron colliders in NNLO QCD*, *Nucl. Phys. B* **646** (2002) 220 [[hep-ph/0207004](#)] [[INSPIRE](#)].
- [27] V. Ravindran, J. Smith and W.L. van Neerven, *NNLO corrections to the total cross-section for Higgs boson production in hadron hadron collisions*, *Nucl. Phys. B* **665** (2003) 325 [[hep-ph/0302135](#)] [[INSPIRE](#)].
- [28] R.V. Harlander and K.J. Ozeren, *Finite top mass effects for hadronic Higgs production at next-to-next-to-leading order*, *JHEP* **11** (2009) 088 [[arXiv:0909.3420](#)] [[INSPIRE](#)].
- [29] S. Marzani, R.D. Ball, V. Del Duca, S. Forte and A. Vicini, *Higgs production via gluon-gluon fusion with finite top mass beyond next-to-leading order*, *Nucl. Phys. B* **800** (2008) 127 [[arXiv:0801.2544](#)] [[INSPIRE](#)].
- [30] R.V. Harlander, H. Mantler, S. Marzani and K.J. Ozeren, *Higgs production in gluon fusion at next-to-next-to-leading order QCD for finite top mass*, *Eur. Phys. J. C* **66** (2010) 359 [[arXiv:0912.2104](#)] [[INSPIRE](#)].
- [31] A. Pak, M. Rogal and M. Steinhauser, *Finite top quark mass effects in NNLO Higgs boson production at LHC*, *JHEP* **02** (2010) 025 [[arXiv:0911.4662](#)] [[INSPIRE](#)].
- [32] A.V. Pak, M. Rogal and M. Steinhauser, *Production of scalar and pseudo-scalar Higgs bosons to next-to-next-to-leading order at hadron colliders*, *JHEP* **09** (2011) 088 [[arXiv:1107.3391](#)] [[INSPIRE](#)].

- [33] R.V. Harlander, T. Neumann, K.J. Ozeren and M. Wiesemann, *Top-mass effects in differential Higgs production through gluon fusion at order α_s^4* , *JHEP* **08** (2012) 139 [[arXiv:1206.0157](#)] [[INSPIRE](#)].
- [34] V. Del Duca, W. Kilgore, C. Oleari, C. Schmidt and D. Zeppenfeld, *Gluon fusion contributions to $H + 2$ jet production*, *Nucl. Phys. B* **616** (2001) 367 [[hep-ph/0108030](#)] [[INSPIRE](#)].
- [35] V. Del Duca, W. Kilgore, C. Oleari, C. Schmidt and D. Zeppenfeld, *Higgs + 2 jets via gluon fusion*, *Phys. Rev. Lett.* **87** (2001) 122001 [[hep-ph/0105129](#)] [[INSPIRE](#)].
- [36] V. Del Duca, W. Kilgore, C. Oleari, C.R. Schmidt and D. Zeppenfeld, *Kinematical limits on Higgs boson production via gluon fusion in association with jets*, *Phys. Rev. D* **67** (2003) 073003 [[hep-ph/0301013](#)] [[INSPIRE](#)].
- [37] J. Alwall, Q. Li and F. Maltoni, *Matched predictions for Higgs production via heavy-quark loops in the SM and beyond*, *Phys. Rev. D* **85** (2012) 014031 [[arXiv:1110.1728](#)] [[INSPIRE](#)].
- [38] K.G. Chetyrkin, B.A. Kniehl and M. Steinhauser, *Decoupling relations to $O(\alpha_s^3)$ and their connection to low-energy theorems*, *Nucl. Phys. B* **510** (1998) 61 [[hep-ph/9708255](#)] [[INSPIRE](#)].
- [39] M. Krämer, E. Laenen and M. Spira, *Soft gluon radiation in Higgs boson production at the LHC*, *Nucl. Phys. B* **511** (1998) 523 [[hep-ph/9611272](#)] [[INSPIRE](#)].
- [40] K.G. Chetyrkin, B.A. Kniehl and M. Steinhauser, *Hadronic Higgs decay to order α_s^4* , *Phys. Rev. Lett.* **79** (1997) 353 [[hep-ph/9705240](#)] [[INSPIRE](#)].
- [41] Y. Schröder and M. Steinhauser, *Four-loop decoupling relations for the strong coupling*, *JHEP* **01** (2006) 051 [[hep-ph/0512058](#)] [[INSPIRE](#)].
- [42] K.G. Chetyrkin, J.H. Kuhn and C. Sturm, *QCD decoupling at four loops*, *Nucl. Phys. B* **744** (2006) 121 [[hep-ph/0512060](#)] [[INSPIRE](#)].
- [43] R. Harlander, T. Seidensticker and M. Steinhauser, *Complete corrections of order $\alpha \alpha_s$ to the decay of the Z boson into bottom quarks*, *Phys. Lett. B* **426** (1998) 125 [[hep-ph/9712228](#)] [[INSPIRE](#)].
- [44] M. Steinhauser, *MATAD: a program package for the computation of MAssive TADpoles*, *Comput. Phys. Commun.* **134** (2001) 335 [[hep-ph/0009029](#)] [[INSPIRE](#)].
- [45] V.A. Smirnov, *Applied asymptotic expansions in momenta and masses*, Tracts in Modern Physics volume 177, Springer, Germany (2002).
- [46] R. Harlander and M. Wiesemann, *Jet-veto in bottom-quark induced Higgs production at next-to-next-to-leading order*, *JHEP* **04** (2012) 066 [[arXiv:1111.2182](#)] [[INSPIRE](#)].
- [47] R. Harlander, <http://www.robert-harlander.de/software/ggh@nnlo>.
- [48] M. Cacciari, G.P. Salam and G. Soyez, *The anti- k_t jet clustering algorithm*, *JHEP* **04** (2008) 063 [[arXiv:0802.1189](#)] [[INSPIRE](#)].
- [49] G. Bozzi, S. Catani, D. de Florian and M. Grazzini, *The q_T spectrum of the Higgs boson at the LHC in QCD perturbation theory*, *Phys. Lett. B* **564** (2003) 65 [[hep-ph/0302104](#)] [[INSPIRE](#)].
- [50] G. Bozzi, S. Catani, D. de Florian and M. Grazzini, *Transverse-momentum resummation and the spectrum of the Higgs boson at the LHC*, *Nucl. Phys. B* **737** (2006) 73 [[hep-ph/0508068](#)] [[INSPIRE](#)].

- [51] D. de Florian, G. Ferrera, M. Grazzini and D. Tommasini, *Transverse-momentum resummation: Higgs boson production at the Tevatron and the LHC*, *JHEP* **11** (2011) 064 [[arXiv:1109.2109](#)] [[INSPIRE](#)].
- [52] S. Catani and M. Grazzini, *An NNLO subtraction formalism in hadron collisions and its application to Higgs boson production at the LHC*, *Phys. Rev. Lett.* **98** (2007) 222002 [[hep-ph/0703012](#)] [[INSPIRE](#)].
- [53] M. Grazzini, *NNLO predictions for the Higgs boson signal in the $H \rightarrow WW \rightarrow l\nu l\nu$ and $H \rightarrow ZZ \rightarrow 4l$ decay channels*, *JHEP* **02** (2008) 043 [[arXiv:0801.3232](#)] [[INSPIRE](#)].
- [54] Z. Nagy and Z. Trócsányi, *Next-to-leading order calculation of four jet observables in electron positron annihilation*, *Phys. Rev.* **D 59** (1999) 014020 [Erratum *ibid.* **D 62** (2000) 099902] [[hep-ph/9806317](#)] [[INSPIRE](#)].
- [55] Z. Nagy, *Next-to-leading order calculation of three jet observables in hadron hadron collision*, *Phys. Rev.* **D 68** (2003) 094002 [[hep-ph/0307268](#)] [[INSPIRE](#)].
- [56] S. Catani and M.H. Seymour, *A general algorithm for calculating jet cross-sections in NLO QCD*, *Nucl. Phys.* **B 485** (1997) 291 [Erratum *ibid.* **B 510** (1998) 503] [[hep-ph/9605323](#)] [[INSPIRE](#)].
- [57] A.D. Martin, W.J. Stirling, R.S. Thorne and G. Watt, *Parton distributions for the LHC*, *Eur. Phys. J.* **C 63** (2009) 189 [[arXiv:0901.0002](#)] [[INSPIRE](#)].
- [58] R.V. Harlander, S. Liebler and H. Mantler, *SusHi: a program for the calculation of Higgs production in gluon fusion and bottom-quark annihilation in the standard model and the MSSM*, *Comp. Phys. Commun.* **184** (2013) 1605 [[arXiv:1212.3249](#)] [[INSPIRE](#)].